Colloidal monolayer self-assembly and its simulation via cellular automaton model*

Wu Yi-Zhi(吴以治), Chen Chen(陈 晨), Xu Xiao-Liang(许小亮)†, Liu Yun-Xi(刘赟夕), Shao Wei-Jia(邵伟佳), Yin Nai-Qiang(尹乃强), Zhang Wen-Ting(张文婷), Ke Jia-Xin(柯佳鑫), and Fang Xiao-Tian(方啸天)

Department of Physics, University of Science and Technology of China, Hefei 230026, *China*

(Received 13 March 2014; revised manuscript received 8 April 2014; published online 20 June 2014)

A wafer-scale colloidal monolayer consisting of SiO_2 spheres is fabricated by a method combining spin coating and thermal treatment for the first time. Moreover, a new cellular automaton model describing the self-assembly process of the colloidal monolayer is introduced. Rather than simulate molecular self-assembly to establish the most energetically favored position, we reconstruct the self-assembly of the colloidal monolayer by adjusting several simple transition rules of a cellular automaton. This model captures the main self-assembly characteristics of SiO_2 spheres, including experimental processing time, morphology, and some statistics. It possesses the advantage of less calculation and higher efficiency, paving a new way to simulate a mesoscopic system.

Keywords: self-assembly, cellular automaton, simulation, colloidal monolayer

PACS: 87.15.A–, 81.16.–c, 81.07.–b, 87.15.nt **DOI:** 10.1088/1674-1056/23/8/088703

1. Introduction

Colloidal crystals have been attracting enormous, widespread interest for its potential applications in plasmonics,[1–3] data storage,[4,5] and photonics.[6–8] A variety of methods, such as floating-transfer methods[9–12] and electric field assisted self-assembly,[13–15] have been developed to create colloidal crystals. However, these methods are capable of building up either colloidal crystal in small domains or requiring strong artificial skills.[9,11,16] Moreover, they seem infeasible for industrial-scale mass-fabrication due to their tedious fabrication processes and incompatibility with wafer-scale batch micro-fabrication, which is widely used in the semiconductor industry.

Spin-coating[17–19] is an alternative strategy to overcome the drawbacks mentioned above. However, there are few reports on using this method to prepare colloidal monolayers. The great challenge is that the spin-coating method is only capable of producing a colloidal monolayer (single crystal) up to 10 μm in length.[19] The obtained colloidal monolayer is still much smaller than industrial size in area and has low-order polycrystallinity. It contains many imperfections including point defects, dislocations, and grain boundaries.[17] In this contribution, we present a self-assembly technique, combining spin coating with thermal treatment, which textures wafer-scale surface areas with monolayer hexagonal close-packed SiO_2 spheres. Through a series of repeated experiments, we find that a wafer-scale colloidal monolayer with few defects can be harvested using thermal treatment. Moreover, we do not need salt or surfactant in solution to assist SiO_2 spheres' self-assembly. We also do not need to charge the particles or introduce confinement between any boundaries or surface pressure control. It is of considerable significance that our procedure is compatible with the semiconductor industry. It worth mentioning here that our newly proposed method has greatly improved the quality of colloidal crystals, although a few defects still exist in the colloidal monolayers because self-assembly is very sensitive to the assembly environment.

The diverse experimental results caused by sensitivity to perturbation of the external environment have led to various models.[20] Computer simulation provides an effective way to validate various models and give qualitative or even quantitative results. However, the simulation of crystallization is a really challenging task, and it has been addressed in only a few publications to date.[21–23] The classical tools used to simulate large molecular systems are deterministic routines such as molecular dynamics, solving Newton's equations of motion,[24] or stochastic algorithms such as the dynamic Monte Carlo method.[25] Skjeltorp's group presented an experimental study of crack growth in a two-dimensional (2D) system, using a monolayer of uniformly sized microspheres confined between two parallel sheets of glass, and simulated the fracture in microsphere monolayers.[23] They are not different from the process of aggregation behavior of SiO_2 spheres. Models of self-assembly based on force field calculations encounter some major problems. (i) Using the description at an atomic level rather than a molecular level makes a simulation more complicated than it needs to be. At such a low level, some unnecessary details make the expression of

*Project supported by the National Natural Science Foundation of China (Grant No. 81172082) and Anhui Provincial Scientific and Technological Project of China (Grant No. 12010202035).

†Corresponding author. E-mail: xlxu@ustc.edu.cn

© 2014 Chinese Physical Society and IOP Publishing Ltd

interactions complex, such as the protein folding problem.[26] (ii) Using a purely mechanistic instead of a cellular automaton modeling technique makes the updating of the system too cumbersome and slower than necessary. For example, in principle, one should make $\sim n^2$ calculations (need to consider every pairwise interaction) in a system with n particles instead of $\sim n$ calculations (just need to consider surrounding neighbors). All of these result in high cost and low efficiency in computing. Consequently, some improved types of molecular dynamics and self-assembly simulation are presented to handle larger molecular systems.[27]

In this paper, we consider the self-assembly of a colloidal monolayer and introduce a simple cellular automaton to simulate the process. We demonstrate that when the system is on the mesoscopic scale ($\sim$ 500 nm) all the detailed physical interactions can be reduced to several simple transition rules of the cellular automaton, and the simulation results are in good agreement with our experimental results. This is the first report on simulating the self-assembly of SiO_2 spheres via a cellular automaton model, and we believe that the study of the simple model can provide insights into more complex systems, many of which are of considerable practical importance.

2. The model for self-assembly of SiO_2 spheres

To simulate a close-packed colloidal monolayer in an experimental simulation system, we introduce a two-dimensional cellular automaton in a hexagonal lattice with data structures representing different occupation states. If one node in a hexagonal lattice is occupied, the state is set to 1, otherwise 0. Given that the number of colloidal crystals during the self-assembly process is constant, conflicting with usual cases in which the total occupation number may vary over time, some adjustments of transition rules should be made. One good solution is to let a sphere propagate to an empty site locally along the edges of a lattice if it satisfies certain rules established according to self-assembly dynamics. Details of transition rules will be described in Subsection 2.3.

2.1. Theoretical background and computer model for self-assembly of SiO_2 spheres

Based on Denkov's[28] and Kralchevsky's[29] work, we introduce the current understanding of the self-assembly mechanism of a colloidal monolayer (Fig. 1). After the substrate with a latex film is placed in an oven for thermal treatment, the spheres in multiple layers are scattered into a monolayer by Brownian motion (Fig. 1(a)). Later, the slightly concave layer thins gradually, owing to liquid evaporation. A 2D crystal nucleus suddenly forms (Fig. 1(b)) when the thickness of the deforming liquid in the center of the substrate becomes equal to the particle's diameter. The surrounding liquid level is higher than that of the center and convective force appears, governing SiO_2 spheres toward the ordered nucleus (Fig. 1(b)). Eventually, a wafer-scale colloidal monolayer forms. Self-assembly of SiO_2 spheres is a process of crystal formation and is thus a phase transition from the viewpoint of thermal dynamics and statistical physics.[30] With thermal treatment, the kinetic energy of the spheres increases, giving them a wider range of movement and promoting their capability to search for the state with the lowest energy. This is the function of thermal treatment on self-assembly for constructing a better colloidal monolayer.

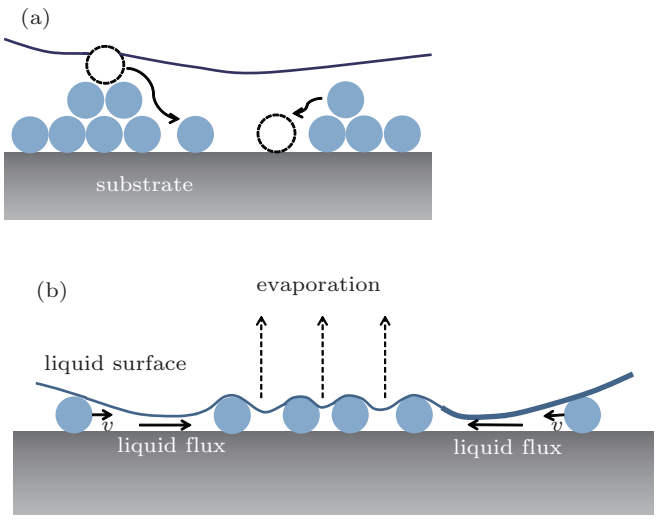


Fig. 1. (color online) Schematic diagram of the mechanism for SiO_2 self-assembly: (a) multiple layers of spheres breaking up into monolayer; (b) initial nucleation and spheres transferring to nucleated areas.

In our experiments, we find that temperature has a significant influence on self-assembly of colloidal monolayer. As the temperature of thermal treatment increases from room temperature (25 °C), multilayered spheres are more likely to be scattered in a monolayer. The liquid evaporates more quickly and the capillary attraction becomes stronger, leading to close-packed spheres. However, an overly high temperature decreases the self-assembly time significantly, which leaves little chance to form the close-packed sphere monolayer. Consequently, moderate temperature (40 °C–60 °C) is needed to acquire a well assembled colloidal crystal. Besides temperature, the volume fraction of latex is another prominent factor affecting the ultimate self-assembly configuration. This is reasonable because there are not enough spheres to cover the whole substrate when the volume fraction of latex is low, whereas multiple layers of spheres would occur when the concentration of latex is overly high.

In order to describe the experimental system, we introduce three self-defining parameters according to the physical process, namely, core rate (CR), threshold (Th), and stop threshold (STh). CR denotes the rate of one colloidal sphere being the nucleus during the self-assembly process, which depends on the temperature of the environment. Th is the initial

ratio of the area occupied by the spheres to the whole substrate area, and we assume Th is proportional to the volume fraction of latex. STh is a given factor that can be calculated by the empirical formula

$$\mathrm{STh} = \mathrm{SL} + (\mathrm{SU} - \mathrm{SL}) \frac{\mathrm{Th} - \mathrm{TL}}{\mathrm{TU} - \mathrm{TL}} \frac{\mathrm{CU} - \mathrm{CR}}{\mathrm{CU} - \mathrm{CL}}.$$

In this formula, TL is the threshold lower limit, TU is the threshold upper limit, CL is the core rate lower limit, and CU is the core rate upper limit, and all of them are determined by tentative simulation. Note that this formula guarantees that STh is within [SL, SU] and linearly dependent on Th and CR. Another self-defining monitor variable in our program is Similarity. It is defined as the ratio of the number of occupied nodes in both adjacent configurations to the number of total occupied nodes in lattice. Similarity stands for the similarity between two adjacent configurations. When it reaches the given STh, the evolvement of the automata will be brought to an end.

2.2. Initial state and boundary condition

In the experiment, several other factors, such as the method of dropping latex on substrates and the components of latex, may influence the initial distribution of the colloidal crystal before self-assembly. Therefore, it makes sense to assume, initially, that nodes of the hexagonal lattice are uniformly occupied with the proportion Th. Similarly, the possibility of one colloidal sphere being the nucleus can be regarded as random. Additionally, it is reasonable to adopt periodical boundary conditions because the simulation scale ($\sim$ 50 μm) is much smaller than the experimental substrate scale ($\sim$ 50 mm).

2.3. Transition rules for self-assembly of SiO_2 spheres

Since self-assembly is the consequence of local interactions between colloidal crystals, taking nearest neighbors into account is reasonable. For the physical mechanism, we set simple transition rules for the cellular automaton. When a colloidal sphere is not connected to a nucleation region, it undergoes Brownian motion, and a biased random walk will be a good model. As for those attached to nuclei, which tend to be close packed, their motions are more likely deterministic.

2.3.1. Transition rule for non-nucleation region

For a non-nucleation region, a bias is added to the equal probabilistic random walk for the transition rule, which is illustrated in Fig. 2.

The transition rules for occupied nodes and unoccupied nodes are shown as follows.

For a quantitative analysis, we calculate additional bias in Fig. 2(a) as

$$\mathrm{bias}_i = \frac{N_i^{\mathrm{nearest}} - \bar{N}^{\mathrm{nearest}}}{\sum_i N_i^{\mathrm{nearest}}}.$$

In this expression, N_i^{nearest} is the number of nearest neighbor spheres of the ith node adjacent to the one being considered, and $\bar{N}^{\mathrm{nearest}}$ is the corresponding mean value. This definition reveals that a colloidal sphere tends to move to the region with a larger-area colloidal crystal and guarantees that its situation is reduced to equal probabilistic cases when every nearest node has the same nearest occupied states.

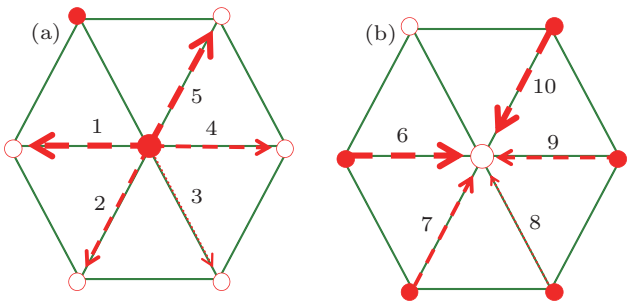


Fig. 2. (color online) Schematic diagram of transition rule for non-nucleation region. Green solid lines denote hexagonal lattice, solid red circles denote occupied nodes, and hollow red circles denote unoccupied nodes. Red dashed arrows with different thicknesses stand for relative transition possibilities. The thicker the arrow is, the greater the possibility is. The thicknesses of arrows in panels (a) and (b) are arrow 1 = arrow 5 > arrow 4 = arrow 2 > arrow 3, and arrow 6 = arrow 10 > arrow 7 = arrow 9 > arrow 8, respectively.

As for unoccupied nodes (Fig. 2(b)), the bias is calculated as

$$\mathrm{bias}_i = -\frac{N_i^{\mathrm{nearest}} - \bar{N}^{\mathrm{nearest}}}{\sum_i N_i^{\mathrm{nearest}}}.$$

2.3.2. Transition rule for nucleation region

When an SiO_2 sphere arrives at a colloidal crystal in a nucleation region, it is more reasonable that it is attached to the nucleation region and inclined to pack closely with others. So the transition rule for these spheres should be deterministic. The occupied node moves toward its nearest nucleus and the unoccupied one moves away from its nearest nucleus. One note is that initial nuclei should remain motionless.

3. Experimental section

3.1. Chemicals and materials

Ammonia solution (AR grade), tetraethyl orthosilicate (AR grade) ethylene glycol ($\geq$ 99.0 wt%) and ethanol ($\geq$ 99.5 wt%) were used as received without further purification. They were purchased from Sinopharm Chemical Reagent Co. (SCRC). Silicon wafers of 1.5 cm $\times$1.5 cm were cleaned according to the RCA procedure[31] and then cleaned in Piranha solution (70% H_2SO_4 + 30% H_2O_2) for 12 h. After this, they were triple cleaned in deionized (DI) water. The resistivity of the water is 18.25 MΩ · cm.

3.2. Fabrication of colloidal monolayer consisting of SiO_2 spheres

Silica spheres were synthetized according to improved Stöber processing.[32,33] The resultant SiO_2 spheres (with diameter of (490 ± 12) nm) were cleaned using three cycles of successive centrifugation and ultrasonic cleaning in ethanol. The purified SiO_2 spheres were re-dispersed in a mixture of ethanol and glycol ($v : v = 1 : 1$) before they were used for spin coating. Then latex samples with volume fraction (VF) of 20% and 40% were prepared for use.

Colloidal latex was deposited on a wafer substrate. The substrate was spin-coated at 550 rpm on a commercial spin coater (CAS, KW-4A) for 9 s to spread the solution to the whole wafer. Thereafter, the substrate was quickly accelerated to 3500 rpm for 30 s. Subsequently, the substrate was transferred to an electric thermostatic drying oven with a quartz window for a certain time. The sample dried from the edge to the center of the substrate gradually. A variety of colors appeared after the latex became dry.

4. Results and discussion

The procedure of spin coating is shown in Fig. 3(a). 50 μL of SiO_2 latex is deposited on a silicon wafer and is spread all over the surface after spin coating under the action of shear force. Some domains with multilayered spheres are inevitable during this process. To improve the quality of the colloid, the sample is immediately transferred to an electric thermostatic drying oven for thermal treatment. When the latex film becomes dry, a monolayer of close-packed spheres forms (Fig. 3(b)).

After some tentative simulation, we established SL = 0.85, SU = 0.99; TL = 0.5, TU = 0.99; CL = 0.01, and CU = 0.07, which correspond well with our experimental system. Based on the transition rules discussed above, we take different temperatures into account. Both the experimental and simulation results are consistent with the following scenario. At early stages, the initial nucleus forms. Then, surrounding spheres transfer to the nucleus. Finally, hexagonal close-packed sphere arrays with large area form. Moreover, figure 4 show that the simulation result is similar to the final distribution of the colloidal monolayer in experiment. Both the experimental results and simulation results are hexagonally close packed and have vacancies and multiple layers of spheres. Additionally, figures 4(a) and 4(e) demonstrate that there are more vacancies and more multilayered spheres at 'low temperature'. Figures 4(b) and 4(f) show that better crystal can be achieved when proper temperature is introduced. Figures 4(c) and 4(g) show that multilayered spheres are fewer at 'high temperature'. However, overly high temperature should be avoided because a lot of vacancies would appear due to the little time left to assemble spheres.

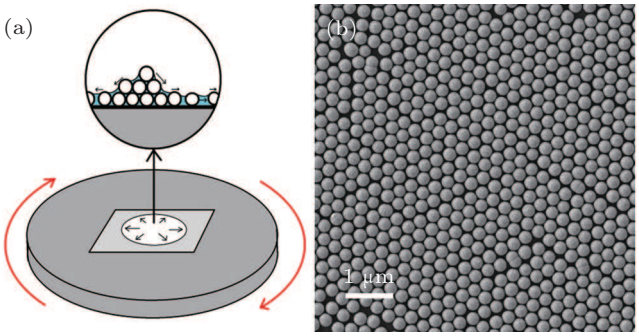


Fig. 3. (color online) (a) A simple cartoon of spin coating; (b) hexagonal close-packed SiO_2 texturing the full substrate under the optimized self-assembly condition of latex VF = 40% and thermal treatment temperature of 45 °C.

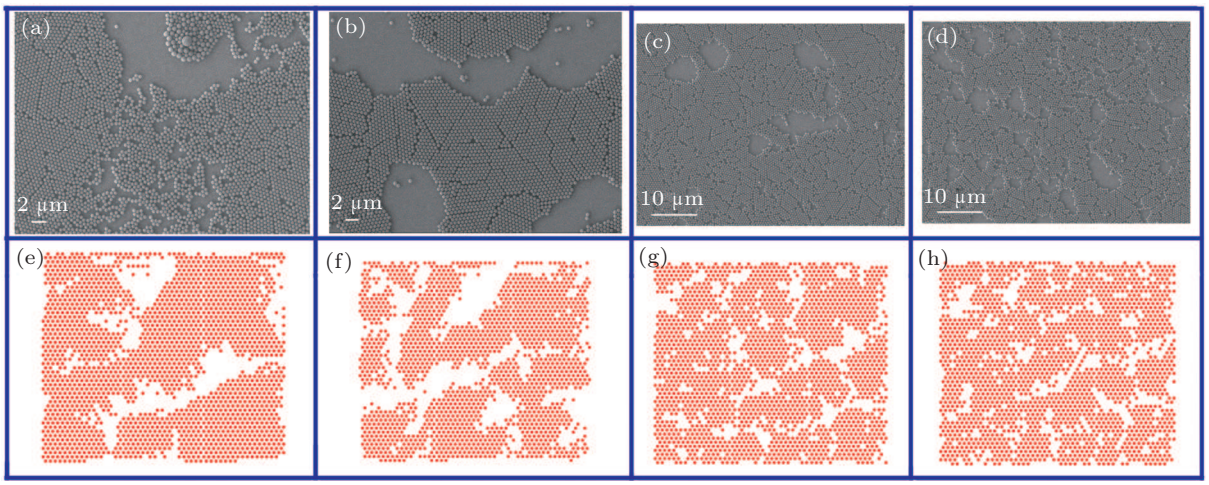


Fig. 4. (color online) SEM images of self-assembly configuration under different temperatures using latex VF of 20% and corresponding simulation results: (a) 25 °C; (b) 45 °C; (c) 65 °C; (d) 85 °C. For simulation, (e) Th = 0.8, STh = 0.934, CR = 0.01; (f) Th = 0.66, STh = 0.879, CR = 0.03; (g) Th = 0.8, STh = 0.878, CR = 0.05; (h) Th = 0.8, STh = 0.85, CR = 0.07. The gridding is 50×50 for all cases.

More detailed information, such as simulation steps (corresponding to self-assembly time) and average areas of vacancy, which both demonstrate the resemblance between experiment and simulation, is shown in Fig. 5. Figure 5(a) reveals that the higher the temperature is, the less self-assembly time is needed, which is easy to understand because high temperature accelerates the liquid evaporation. Moreover, figure 5(b) reveals that the simulation results are quite consistent with the experimental results. In our simulation, some sphere groups are considered as one cluster even though there is only one sphere connecting them, and these obviously should be regarded as separate clusters. To overcome this problem, we analyzed the vacancy area and found the interesting fact that vacancy areas are small at both high and low temperature. As the temperature increases, the trend of vacancy numbers in Fig. 5(b) appears like a parabola. At low and high temperatures, the value of average vacancy numbers is low, which indicates that the SiO_2 spheres are packed with low order. It is reasonable that the spheres can be mostly close packed under optimal temperature, leaving behind the largest vacancy areas.

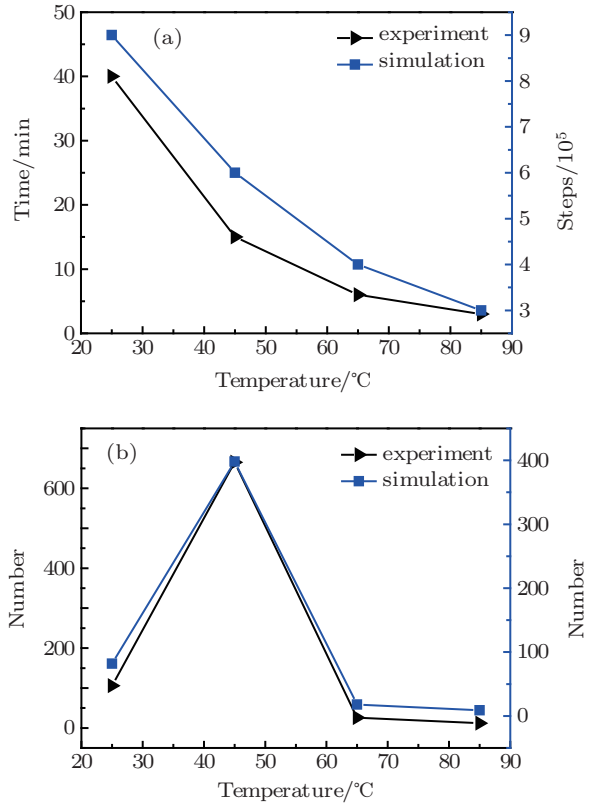


Fig. 5. (color online) The characterization of the simulation and experiment: (a) self-assembly time in experiment and evolvement steps in simulation; (b) average vacancy numbers (equal to the vacancy areas divided by the vertical projection area of a single sphere) for experiment, and numbers of vacancy grids for simulation.

Our simple cellular automaton can also handle cases with different volume fractions of latex, which is demonstrated in Fig. 6. The morphology of simulation results is very much in accordance with the experimental results. When the latex volume fraction is 20% more than half the area of the sample is covered with a colloidal monolayer, and the spheres precisely cover the whole substrate when the latex concentration increases to 40%.

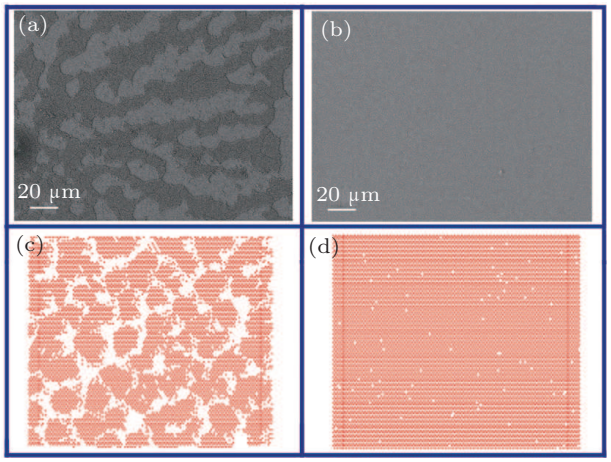


Fig. 6. (color online) SEM images of self-assembly configurations with different latex volume fractions and corresponding simulation results: (a) 20%; (b) 40%. For simulation, (c) Th = 0.7, STh = 0.887, CR = 0.03; (d) Th = 0.99, STh = 0.941, CR = 0.03. The gridding is 100 × 100 for all cases.

5. Conclusion

We have demonstrated the formation of a high-quality, wafer-scale colloidal monolayer using our proposed method, namely thermally assisted self-assembly of silica spheres. Moreover, we improved the traditional self-assembly theory. Based on this mechanism, a simple cellular automaton is employed to simulate the self-assembly process for the first time. It is demonstrated that, even when detailed physical interactions are reduced to a few simple transition rules, a cellular automaton simulation can still yield good agreement with experimental results. This may be promising due to its low computing cost and high efficiency, paving a new path to simulation of self-assembly in mesoscopic systems and investigation of its internal dynamics. Moreover, this approach is highly compatible with contemporary micro-fabrication, so it may eventually enable mass production of low-cost practical devices for applications including nano-lithography, photonics, data storage, biosensors, and plasmonics.

References

[1] Vogel N, Jung M, Bocchio N L, Retsch M, Kreiter M and Koper I 2010 *Small* **6** 104
[2] Xue W R, Guo Y N and Zhang W M 2009 *Chin. Phys. B* **18** 2529
[3] Pan D, Wei H and Xu H X 2013 *Chin. Phys. B* **22** 097305
[4] Betzig E, Trautman J K, Wolfe R, Gyorgy E M, Finn P L, Kryder M H and Chang C H 1992 *Appl. Phys. Lett.* **61** 142
[5] Sun S H, Murray C B, Weller D, Folks L and Moser A 2000 *Science* **287** 1989
[6] Marlow F, Muldarisnur, Sharifi P, Brinkmann R and Mendive C 2009 *Angew. Chem. Int. Ed.* **48** 6212
[7] Galisteo-Lopez J F, Ibisate M, Sapienza R, Froufe-Perez L S, Blanco A and Lopez C 2011 *Adv. Mater.* **23** 30

[8] Zhang L F and Huang J P 2010 *Chin. Phys. B* **19** 024213
[9] Lenzmann F, Li K, Kitai A H and Stover H D H 1994 *Chem. Mater.* **6** 156
[10] Cho Y H, Cho G and Lee J S 2004 *Adv. Mater.* **16** 1814
[11] Ctistis G, Patoka P, Wang X, Kempa K and Giersig M 2007 *Nano Lett.* **7** 2926
[12] Wang Y, Rybczynski J, Wang D and Ren Z 2005 *Nanotechnology* **16** 819
[13] Fudouzi H, Kobayashi M and Shinya N 2002 *Adv. Mater.* **14** 1649
[14] Aizenberg J, Braun P V and Wiltzius P 2000 *Phys. Rev. Lett.* **84** 2997
[15] Li C R, Li S W, Mei J, Xu Q, Zheng Y Y and Dong W J 2011 *Chin. Phys. B* **20** 078102
[16] Xia Y N, Gates B, Yin Y D and Lu Y 2000 *Adv. Mater.* **12** 693
[17] Deckman H W and Dunsmuir J H 1982 *Appl. Phys. Lett.* **41** 377
[18] Dux C and Versmold H 1997 *Phys. Rev. Lett.* **78** 1811
[19] Fischer U C and Zingsheim H P 1981 *J. Vac. Sci. Technol.* **19** 881
[20] Lehn J M 2002 *Science* **295** 2400
[21] Rabani E, Reichman D R, Geissler P L and Brus L E 2003 *Nature* **426** 271
[22] Ku J Y, Aruguete D M, Alivisatos A P and Geissler P L 2011 *J. Am. Chem. Soc.* **133** 838
[23] Skjeltorp A T and Meakin P 1988 *Nature* **335** 424
[24] Vangunsteren W F, Luque F J, Timms D and Torda A E 1994 *Ann. Rev. Bioph. Biom.* **23** 847
[25] Kirkpatrick S, Gelatt C D and Vecchi M P 1983 *Science* **220** 671
[26] Böhm G 1991 *Chaos, Solitons and Fractals* **1** 375
[27] Mayer B, Kohler G and Rasmussen S 1997 *Phys. Rev. E* **55** 4489
[28] Denkov N D, Velev O D, Kralchevsky P A, Ivanov I B, Yoshimura H and Nagayama K 1992 *Langmuir* **8** 3183
[29] Kralchevsky P A and Nagayama K 1994 *Langmuir* **10** 23
[30] Wu Y Z, Zhang C, Yuan Y, Wang Z W, Shao W J, Wang H J and Xu X L 2013 *Langmuir* **29** 14017
[31] Skidmore K 1987 *Semiconductor International/Semiconductor International* **10** 80
[32] Stober W, Fink A and Bohn E 1968 *Journal of Colloid and Interface Science* **26** 62
[33] Wu Y Z, Ren S M, Xu X L, Liu L, Wang H J and Yu J 2014 *Solar Energy Materials and Solar Cells* doi: 10.1016j.solmat.2014.03.050